Communications in Computational Chemistry
Commun. Comput. Chem., Vol. 7, No. 4, 331–342
doi: 10.4208/cicc.2025.146.01

Regular Article

Breathing New Life into Classical Force Fields

Xiwen Sun[1,2], Xueguang Shao[1,2,3], Wensheng Cai[1,2,3,*] and Haohao Fu[1,2,3,*]

[1]*Research Center for Analytical Sciences, Tianjin Key Laboratory of Biosensing and Molecular Recognition, State Key Laboratory of Medicinal Chemical Biology, College of Chemistry, Nankai University, Tianjin 300071, China;*

[2]*Haihe Laboratory of Sustainable Chemical Transformations, Tianjin 300192, China;*

[3]*School of Materials Science and Engineering, Smart Sensing Interdisciplinary Science Center, Nankai University, Tianjin 300350, China.*

[*] Corresponding authors: fhh2626@nankai.edu.cn (H.F.), wscai@nankai.edu.cn (C.C.)

Received on 26 May 2025; Accepted on 24 June 2025

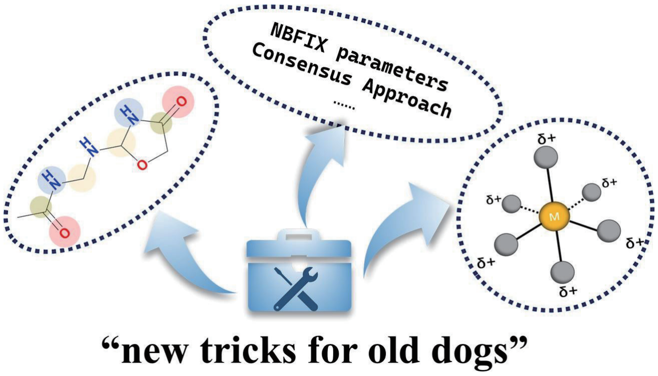

Abstract: Classical force fields form the foundation of molecular dynamics simulations. Because classical force fields are limited to pairwise-additive Lennard-Jones potentials and fixed-charge electrostatics, they cannot accurately capture explicit polarization and charge-transfer effects, metal coordination bonds, or weak, directional nonbonded interactions such as π–π stacking. Machine-learning force fields and polarizable force fields, which have been claimed to accurately characterize these types of interactions, have developed rapidly in recent years, raising an ongoing debate over whether further improvements to classical force fields are still necessary. Keeping this question in mind, we review various strategies proposed in recent years to improve the description of nonbonded interactions for classical force fields. These advances include the development of atomic charge models that accurately reflect molecular dipoles, water models that capture electrostatic screening and solvation effects, atom-pair-specific van der Waals parameters to mimic polarization, refined atom types that better represent chemical environments, and the introduction of virtual sites for accurately modeling of lone pairs. We also discuss the applicable scope of each strategy. Furthermore, by comparing classical force fields with polarizable and machine-learning-based force fields, we identify three major advantages of classical force fields: high computational efficiency, strong transferability, and ease of parameterization. Therefore, we join the ongoing debate and believe that the community will greatly benefit from further development of classical force fields. Through the improvement of the accuracy of characterizing nonbonded interactions, classical force fields can be widely applied in areas such as million-atom simulations and high-throughput screening.

Key words: force fields, polarization, charge transfer nonbonded interactions.

1. Introduction

Molecular Dynamics (MD), as a vital tool in the field of computational chemistry, fundamentally relies on the physical accuracy of force fields to ensure the reliability of simulation results [1-8]. Although mainstream classical, or fixed-charge, force fields such as AMBER [9,10], CHARMM [11,12] and OPLS [13,14] have undergone decades of parameter optimization and have achieved remarkable success in biomolecular simulations such as protein folding and drug design, [9,15-18] their accuracy in describing certain types of nonbonded interactions remains a subject of debate. It is generally believed that [15], due to the limitations of the functional form of classical force fields, phenomena such as charge transfer, polarization effects, metal coordination, and π–π interactions cannot be accurately captured [19-25]. A common viewpoint holds that the accurate description of such types of interactions requires either the introduction of new functional terms, usually the polarization term, into classical force fields or a shift toward more complex machine-learning-based models [26-36]. Therefore, models such as 12-6-4 [37,38], AMOEBA [32,34,39,40], Drude [41,42], ANI [43], Deep Potential [44] and NN PES [45] have been proposed. Despite the great success of these potentials, their application in the study of complex biochemical processes remains severely limited due to constraints in computational efficiency and software implementation, and difficulties in parameterization, especially for systems involving more than 100,000 atoms or tasks that require high-throughput simulations [20,44,46].

Recent studies have found that by employing “new tricks for old dogs”, which are methods that improve the accuracy but do not change functional form of classical force fields, nonbonded interactions such as charge transfer, polarization, coordination, and π–π stacking can be accurately mimicked. Since these new techniques do not alter the functional form of classical force fields, they can serve as drop-in replacements for widely used force fields such as CHARMM [11] and AMBER [9,10] in any molecular dynamics engine, without incurring additional computational costs. As a result, these methods offer a practical way to improve the accuracy of potential energy surface descriptions in MD simulations and can be broadly applied to model a wide range of complex biochemical processes. However, because end users typically rely on default parameter files provided by MD engines, such improvements and newly developed force field parameters have not received widespread attention, adoption, or discussion.

Therefore, this paper focuses on the description of nonbonded interactions by classical force fields, reviews recent strategies proposed to improve their accuracy, and discusses their applicability. We highlight the importance of adopting these new methods and newly published parameters, and provide practical guidance for end users. By comparing classical force fields with polarizable and machine-learning-based force fields, we emphasize the continued relevance of advancing classical force field development. Furthermore, we offer perspectives on future directions for classical force fields. The outline of this review is shown in Figure 1.

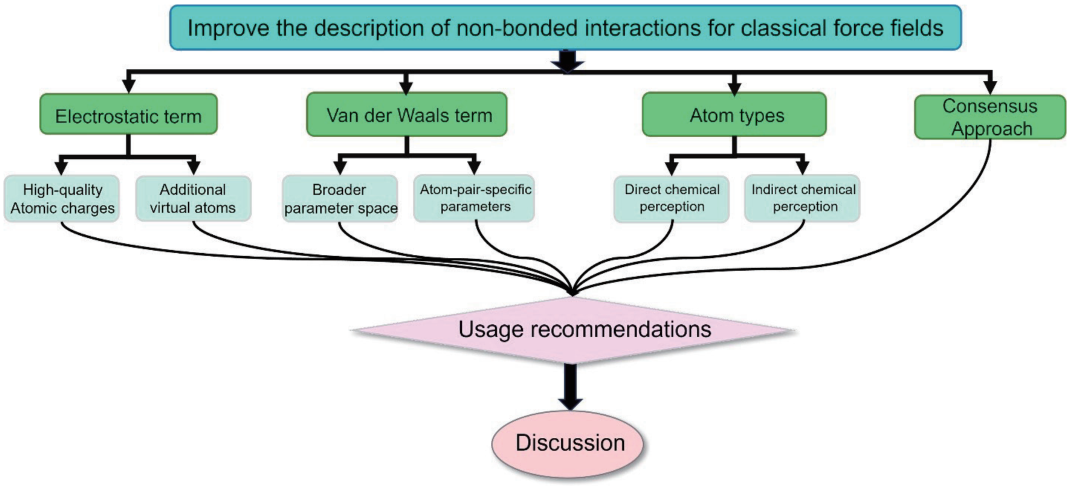

Figure 1. Outline of this review.

Functional form of classical force fields and the types of interactions they fail to describe

In classical force fields, the calculation of potential energy is decomposed into two parts: bonded and nonbonded interactions:

$$E_{\text{total}} = E_{\text{bonded}} + E_{\text{nonbonded}}$$

The functional equation for the nonbonded interaction is:

$$E_{\text{nonbonded}} = \sum_{ij} \frac{q_i q_j}{4\pi\varepsilon r_{ij}} + \sum_{ij} \varepsilon_{ij}\left[\left(\frac{\sigma_{ij}}{r_{ij}}\right)^{12} - 2\left(\frac{\sigma_{ij}}{r_{ij}}\right)^{6}\right]$$

For different atom types, the calculation of van der Waals interactions requires combination rules. For example, CHARMM and Amber force fields follow the Lorentz-Berthelot combination rule [47,48]:

$$\sigma_{ij} = (\sigma_{ii} + \sigma_{jj})/2$$
$$\varepsilon_{ij} = \sqrt{\varepsilon_i \varepsilon_j}$$

In classical force fields, Coulomb’s law characterizes charge–charge, charge–dipole, and dipole–dipole interactions between molecules [49,50]. In contrast, the physical meaning of the 12-6 potential remains somewhat controversial, as it was originally proposed primarily for computational convenience [51,52]. Chipot’s group and Merz’s group have pointed out that the 12-6

Lennard-Jones potential describes Pauli repulsion and induced dipole–induced dipole interactions [37,53]. However, it fails to accurately capture charge–induced dipole and dipole–induced dipole interactions. To model these latter interactions correctly, an additional r^{-4} term has been proposed to be incorporated into the force field [54,55]. Moreover, since atomic charges are fixed in classical force fields, this electrostatic energy representation does not describe charge transfer effects that arise from the redistribution of electron density in response to environmental changes [21,56,57].

Due to the inherent limitations of classical models in handling interactions relevant to induced dipole and charge transfer, they face a range of challenges in accurately describing the complex interactions present in real molecular systems. These issues are particularly pronounced in specific cases such as solutes affected by a high polarizing solvent, coordination complexes involving transition metal ions, π–π stacking in aromatic systems, directional halogen bonding, and salt-bridge interactions [20,58-61]. For example, transition metal ions and ligands typically form coordination bonds accompanied by electron density redistribution and charge transfer, which are difficult for traditional fixed-charge models to capture [54,58] Meanwhile, π–π stacking interactions between aromatic molecules induce significant polarization effects that are also considered challenging to describe accurately using classical models [62].

2. Improvements in the electrostatic term

High-quality atomic charges. Since classical force fields use Coulomb's law to approximate charge-charge, charge-dipole, and dipole-dipole interactions between molecules, intuitively, atomic charges obtained by fitting the electrostatic potential around a molecule in a vacuum environment (e.g., MK, CHELPG, etc.) accurately reflect the interactions between rigid-body-like molecules and surrounding molecules [63-65]. However, since molecular simulations are usually performed in condensed phase, the solute molecule becomes polarized by the surrounding solvent. Classical force fields have difficulty reflecting this phenomenon due to their fixed-charge property. Traditionally, quantum chemistry methods that overestimate the vacuum molecular dipole (e.g., Hartree-Fock) are employed to calculate the atomic charge for compensating for the underestimate of solvent polarization [66]. This strategy, however, lacks theoretical rigor and often results in over-polarization [10,67,68]. To address this problem, Gilson's group proposed the RESP2 charge [69].

$$q_i^{\mathrm{RESP2}} = (1-\delta)\, q_i^{\mathrm{gas}} + \delta q_i^{\mathrm{sol}}$$

where q_i^{gas} and q_i^{sol} are the atomic charges calculated by high-accuracy quantum chemical methods in vacuum and in solution, respectively, and δ is an adjustable parameter that can be optimized by fitting experimental data. By balancing the atomic charges calculated in vacuum and in solution, the RESP2 charge can accurately consider the polarization effect of the solvent on the solute molecules and enhances the accuracy of the classical force-field model in describing condensed-phase systems. Compared with the conventional RESP charge, the force field with the RESP2 charge more accurately reflects the physical properties, including evaporation enthalpy, density, free energy of dissolution, and dipole moment of molecules in solution. Compared to RESP2 charge, 1.2*CM5 and 1.14*CM1A-LBCC adopt a charge scaling method to reflect the polarization effect of the environment on the molecules, which is slightly less physically rigorous but simpler to calculate [70, 71].

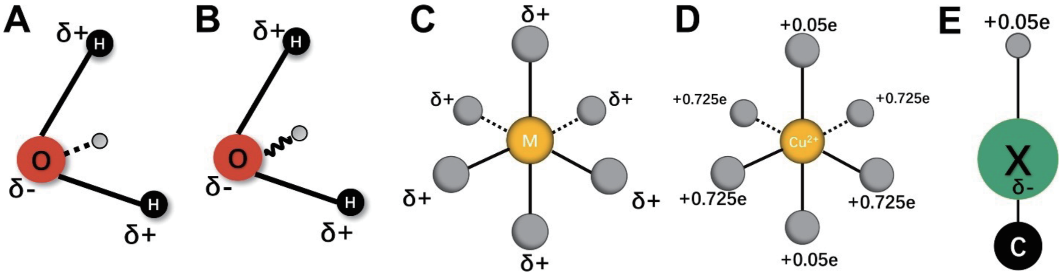

Figure 2. A selection of advanced models for molecular simulations. (A) TIP4P water model, which features fixed partial charges and rigid geometry; (B) OPC3-pol model, which introduces a heavy virtual particle to capture polarizability in a computationally stable manner; (C) octahedral dummy atom model proposed by Åqvist and Warshel, designed to mimic transition metal–ligand coordination environments; (D) Cu-Dum model, which employs asymmetric dummy charges to reproduce the Jahn–Teller distorted hydration structure of Cu^{2+}; and (E) directional σ-hole model, utilizing a positively charged virtual site to represent halogen bonding.

Additional virtual atoms. In most MD simulations, water is not only the most common solvent environment, but also a key determinant of the behavior of solutes [72-74]. Recent three-point water models (e.g., TIP3P-FB and OPC3) can accurately reproduce various physical properties of water, including density, dielectric constant, surface tension, self-diffusion coefficient, etc., thereby improving the physical realism of biomolecular simulations [75-78]. However, because these models are often too simple and do not explicitly describe the lone pairs of water molecules, they may not accurately characterize the polarization effect and charge-shielding behavior of water [41,79]. The TIP4P force field is perhaps the first model that proposes mimicking lone pairs by using dummy atoms to improve the ability of the classical force fields to describe the properties of small molecules (Figure 2A) [80]. In recent years, the TIP4P-FB and OPC force fields accurately reflect various physicochemical properties of water, including the dielectric constant, thus accurately describing the shielding behavior of water for classical interactions between solute molecules [75,81]. Tests on protein systems show that the combination of the Amber ff19SB force field and the OPC model accurately describes the thermodynamic and kinetic behavior of biological macromolecules [10].

In addition, to solve the problem that the classical water model cannot reflect the polarization response of water molecules, Xiong et al. proposed a water model, OPC3-pol (Figure 2B), under the framework of classical force fields, which is capable of describing polarization interactions [82]. The core design objective of this model is the introduction of a charged virtual atom to mimic the polarization effect [82]. Unlike conventional polarizable force fields such as Drude [83], OPC3-pol uses charged virtual atoms of large mass connected to oxygen atoms via harmonic bonds. This approach allows the use of the exact same functional form and integration algorithms as the classical force field, avoiding the computational instability and additional algorithmic overheads introduced by the near-zero particle mass in the conventional polarizable models. In contrast to previous polarizable models, OPC3-pol achieves a stable polarization response through the large mass of virtual atoms and strong force constants, avoiding the "polarization catastrophe" while ensuring energy stability at standard 2 fs (or even 4 fs) time steps. This strategy makes OPC3-pol compatible with classical force fields and applicable to routine biomolecular simulations, significantly lowering the difficulty for the practical use of polarization models while maintaining an accurate description of polarization [82].

Apart from the lone-pair donors such as water, accurately describing the lone-pair acceptors such as metal ions is also very important [84]. It has been found that when using classical force fields to model metal ions in aqueous solution, it is difficult to accurately reproduce both the ion-oxygen coordination distances and the solvation free energies. To address this issue, Åqvist and Warshel have proposed the octahedral dummy atom model, which uses six fractionally charged dummy atoms surrounding the metal center in an octahedral configuration to mimic the orbital hybridization of the metal ions in the formation of coordination bonds (Figure 2C) [85]. Fernanda Duarte et al. have improved on this by systematically optimizing the van der Waals parameters and charge distributions, and have proposed Mn^{2+}, Zn^{2+}, Mg^{2+} and Ca^{2+}, Ni^{2+}, Co^{2+} and Fe^{2+} dummy-atom model parameters [85]. Using two common water models, TIP3P and SPC, tests show that dummy-atom models reproduce both the experimental solvation free energies and metal-water coordination distances. In addition, the accuracy of dummy-atom models has been proven by simulations of a variety of metalloenzyme systems [86,87]. In brief, dummy-atom models provide a reliable solution for the accurate modeling of transition metal systems in classical MD simulations.

On the basis of normal dummy-atom models, Liao et al. have developed the first nonbonded Cu^{2+} model that characterizes the Jahn-Teller effect. Given that Cu^{2+} exhibits typical axial-equatorial coordination asymmetry in water (i.e., the Jahn-Teller effect), it is difficult to accurately reproduce its structural features and hydration thermodynamic properties with classical point-charge models. To solve this problem, the authors designed a compressed octahedral geometry in which the dummy atoms on the equatorial plane have a high positive charge (+0.725e) and the axial dummy atoms have a low charge (+0.05e) to show a greater attraction to the equatorial ligands compared to the axial coordinating ligands. This model successfully reproduces the experimental coordination structure ($\text{Cu-O}_{eq} \approx 1.94$ Å, $\text{Cu-O}_{ax} \approx 2.26$ Å) and solvation free energy (-496.1 kcal/mol) of Cu^{2+} in several metalloprotein systems. This result suggests that the dummy-atom models have the versatility and physical reliability to accurately characterize a variety of transition metal ions [58].

Describing halogen bonds using classical force fields is challenging because overall negative charges are usually assigned to halogen atoms. These force fields are thus unable to delineate the regions of positive electronegativity along the covalent bonding axes, making it difficult to simulate the directional attraction typical of halogens and electron donors [88,89,90]. To address this issue, Gutiérrez et al. have introduced the σ-hole virtual particle model in the CHARMM generalized force field (CGenFF) framework [60,91] to simulate the electrical anisotropy of halogen atoms by adding positively charged virtual particles along the extended line of the C-X bond axis of the halogen atom (Figure 2E) [60]. The positions of the virtual particles, the charge magnitudes, the charge distributions of the halogen atoms and their attached carbon atoms, and the Lennard-Jones parameters have been systematically optimized [60]. The interaction energy profiles of modeled haloaromatics with water, acetone, and N-methylacetamide have been examined using quantum chemical calculations as a reference and further calibrated via multi-target fitting to experimental liquid-phase properties (e.g., enthalpy of evaporation, molecular volume) versus relative solvation free energies ($\Delta\Delta G_{\text{hydr}}$). The method has been validated for its applicability and generality in a variety of protein-ligand complex systems, demonstrating that adding virtual atoms may be a generally applicable method to improve the ability to describe interactions that are not well characterized by classical force fields.

3. Improvement of the van der Waals term

Exploring broader parameter space. As the use of dummy-atom models to characterize metal ions may present technical difficulties for non-specialists, methods to enhance the description of point-charge models for metal ions by improving the van der Waals term are still explored. Toward this end, Li et al. have proposed a systematic parameter-optimization strategy for optimizing the van der Waals parameters of point-charge ion models [55]. However, they concluded that a computationally cheap r^{-4} term must be added to the force field for the metal ions to accurately characterize both the solvation free energies and ion-oxygen distances in aqueous solution (Figure 3A and 3B) [55]. To address this issue, Zhang et al. have proposed that the range of values of the Lennard-Jones parameters can be extended to one that is traditionally considered unphysical [92]. By doing this, Zhang et al. show that the classical 12-6 point-charge model can be used to accurately reproduce both the solvation free energies and ion-oxygen distances of metal ions without the need to introduce additional functional terms and dummy atoms (Figure 3B). This strategy shows that the point-charge ion model can achieve an accuracy comparable to the dummy-atom model in some cases, while maintaining parameter simplicity and model generality [92]. The method provides a drop-in solution for achieving accurate metal ion description in classical force fields. It should be pointed out that, because the parameters of Zhang et al. are considered unphysical, their transferability to different molecular assemblies may not match that of dummy-atom or 12-6-4 models [93]. End users should validate the parameters before use; otherwise, they may adopt safer alternatives [94-98].

Atom-pair-specific van der waals parameters. One of the drawbacks of classical force fields is that they do not characterize the polarization effects in different chemical microenvironments through simple combination rules [6,11,80,99]. For instance, the commonly used Lorentz-Berthelot combination rule is only a simple arithmetic or geometric average of the van der Waals parameters of two different types of atoms, which obviously cannot describe polarization in various complex chemical environments.

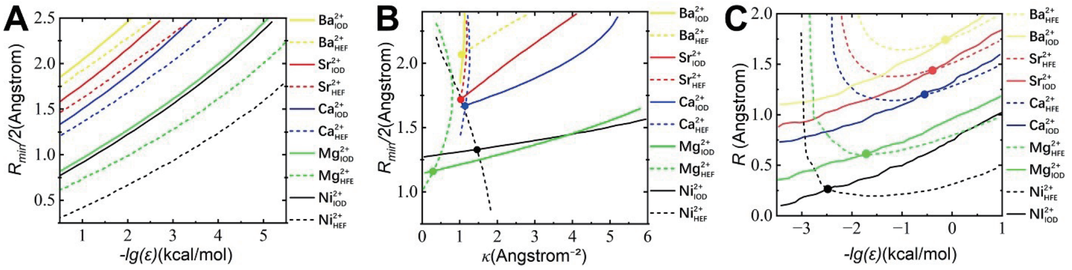

Figure 3. Determination of optimal Lennard-Jones parameters. Dashed lines represent parameter sets capable of yielding solvation free energies consistent with experimental values, while solid lines represent parameter sets capable of yielding ion–oxygen distances consistent with experimental values. The intersection of the dashed and solid lines indicates the optimal parameters for the ions. (A) In the parameter range that is generally regarded as physically sound, the solid and dashed lines do not intersect, suggesting that classical point-charge force fields may not accurately describe metal ions. (B) An improved model proposed by Li et al [55]., in which an additional r^{-4} term is incorporated into the 12-6 potential to account for ion–induced dipole interactions. This modification makes it possible to reproduce both solvation free energies and ion–oxygen distances. The horizontal axis represents κ, a parameter that defines the strength of the r^{-4} term in the 12–6–4 Lennard-Jones nonbonded model. (C) An alternative approach proposed by Zhang et al [92]. By considering a range of values for the Lennard-Jones parameters that is traditionally considered unphysical, the original 12-6 formulation enables the accurate reproduction of both solvation free energies and ion–oxygen distances without introducing extra functional terms.

To address this issue, a strategy for fine-tuning nonbonded interactions by atom-pair-specific corrections (nonbonded fix, NBFIX) can be used. This strategy allows deviation from combination rules by providing the van der Waals parameters (*ε* vs. $r_{\min}$) directly for specific atom pairs. Obviously, this method allows atoms in different microenvironments to interact distinctly, therefore mimicking polarization. As an example, Luo et al. have proposed the NBFIX parameters for Na^+ and K^+ interactions with Cl- by fitting the experimentally obtained osmotic pressures [100]. Sengupta et al. studied the chelate effect of Cd^{2+} complexes using NBFIX-based parameters [98].

The overall description of biomolecules by classical force fields can be improved by systematically providing NBFIX parameters for atom pairs in various chemical environments within biomolecules. The CUFIX force field systematically improves the description of amine-carboxylate, amine-phosphate, and aliphatic carbon-carbon interactions for the CHARMM and Amber force fields [101], and the HB-CUFIX force field further extends the improvement to hydrogen bonding in RNA [102]. The CHARMM36-WYF force field improves the description of cation-*π* indole-choline and indole-trimethylated lysine interactions in the CHARMM 36 force field [103]. To accurately account for the contribution of water in the NBFIX parameterization process, we have proposed a strategy to optimize the van der Waals parameters based on quantum mechanics/molecular mechanics (QM/MM) potential-of-mean-force (PMF) calculations [61,62,104,105]. This approach fully takes into account the effect of hydration-shell water on the interactions when fitting the parameters. The obtained parameters, therefore, can accurately describe of the specific interactions in the aqueous environment [62]. We have proposed CHARMM36m-NBF and CHARMM36m-SBF force fields based on this strategy, which systematically improve the description of all cation-*π* and salt-bridge interactions in biomolecules (Figure 4) [61, 62]. Compared with the classical CHARMM36m force field, the CHARMM36m-NBF and CHARMM36m-SBF force fields enhance the accuracy

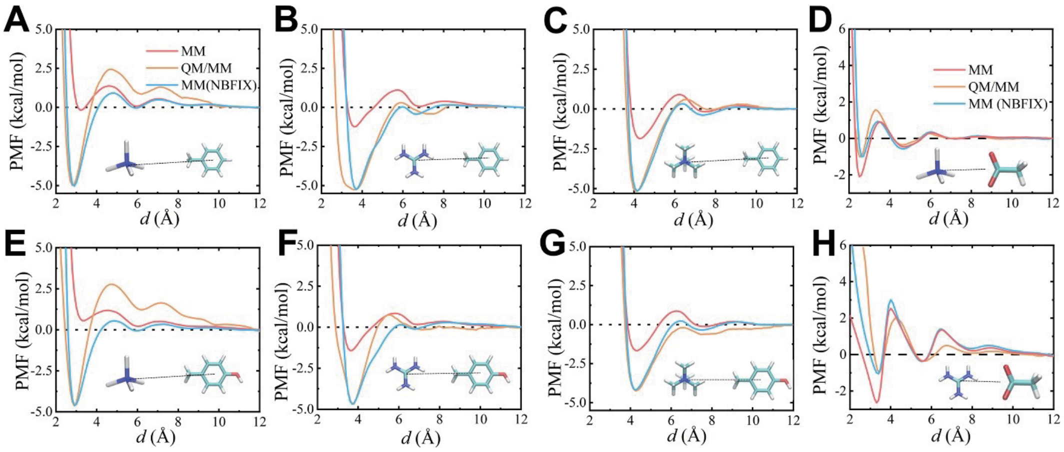

Figure 4. Parameterization of CHARMM36m NBF/SBF force fields using QM/MM PMF calculations for diverse biologically relevant interactions. (A–C and E-G) Cation–*π* interactions: (A) NH_4^+–toluene, (B) Gua^+–toluene, (C) TMA^+–toluene, (E) NH_4^+–p-cresol, (F) Gua^+–p-cresol, (G) TMA^+–p-cresol; (D and H) Salt-bridge interactions: (D) ammonium–acetate, (H) guanidinium–acetate. Results show that NBFIX- and SBF-corrected models yield PMFs that are in significantly better agreement with QM/MM references compared with the standard CHARMM36m force field, suggesting the remarkable accuracy of the former across different interaction types.

of absolute binding free-energy calculations of protein-ligand complexes, the prediction of intrinsically disordered protein structures, and the investigation of Trp-cage folding paths, without any additional computational cost [61,62,106-108]. Therefore, the NBFIX-based strategy effectively enhances the accuracy of the classical force field in describing interactions in different chemical environments without changing the functional form of the force field, and it can be used as a drop-in solution for simulations of a variety of molecular assemblies.

4. More atom types

Indirect chemical perception. Disregarding the NBFIX-based improvements, classical force fields describe atomic properties in different chemical environments by defining distinct atom types—a strategy known as indirect chemical perception (ICP) (Figure 5) [109]. In the same spirit of NBFIX parameters, the more atom types, the more accurately different chemical environments a force field describes. Boulanger et al. demonstrated that by introducing more fine-grained atom types into the GAFF force field and re-optimizing the van der Waals parameters for each type, the accuracy of small-molecule solvation free energy calculations can be significantly improved [110]. The OPLS3 force field, along with its successors OPLS4 and OPLS5, greatly enhanced the description of small molecules in classical force fields by dramatically expanding the number of atom types to cover as much of the chemical space as possible [111-113]. This improvement in turn leads to more accurate predictions of protein–ligand binding free energies [110]. In recent years, machine learning has also been introduced to automate atom type recognition. For example, Zhang et al. employed a topology-aware graph convolutional network (TAGCN [114]) to predict atom types based on atomic environments, achieving over 90% accuracy [115]. These approaches, similar to the NBFIX-based strategy, improve the ability of describing distinct interactions in different chemical environments without changing the functional form of classical force fields.

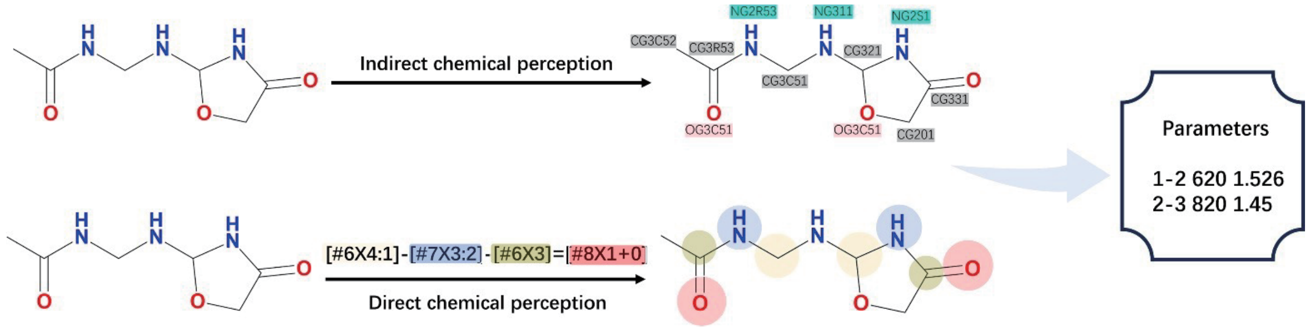

Figure 5. A schematic comparison of the ICP and DCP workflows for determining of force field parameters of a drug-like molecule.

Direct chemical perception. ICP presents some inherent problems: to ensure the accuracy of the parameter calls, the atom types often need to be defined in an extremely complex way, which leads to the expansion of the parameter library size and many redundant parameters, thereby increasing the complexity of the force field and the difficulty of optimization [116-119]. To solve this problem, Mobley et al. have proposed a strategy called Direct Chemical Perception (DCP) [109]. Instead of using atom types, this approach matches substructures of the chemical environments of atoms directly on molecular chemical maps using the industry-standard SMARTS/SMIRKS model, where each parameter (e.g., bond lengths, bond angles, dihedral angles, and Lennard-Jones potentials) is independently assigned by matching a specific chemical substructure (Figure 5). In other words, the DCP method proposes a corresponding atom type for each chemical environment. This pattern matching employs prioritization to select only the substructure rule that matches the most specific substructure, thus explicitly transforming the chemical information that is originally implied in the atom types into clear matching rules, effectively avoiding technical difficulties such as type redundancy, parameter overlap, and context dependency. A force field framework based on the DCP strategy with the SMIRNOFF format as the core, OpenFF, has been developed [109]. Through direct chemical sensing, the OpenFF force field achieves significant improvements in the accuracy of structure optimization, the accuracy of relative conformational energies, and the prediction performance of physical properties (e.g., solvation free energies, transfer free energies). It should be noted that some machine-learning approaches can be regarded as a special type of DCP. For example, the Espaloma model bypasses the conventional atom typing process altogether by using a message-passing neural network to directly map molecular topology to force field parameters, thereby significantly improving modeling accuracy for small molecules and ligand systems [120]. By functioning like ICP with infinite atom types, DCP offers a significant enhancement in how classical molecular force fields describe interactions within diverse environments, positioning it for widespread application in the study of organic small molecules.

5. Consensus approach

In the absence of a priori knowledge, it is uncertain which force field gives the most accurate results for the molecular assembly under study. At this point, the consensus approach can be used to reduce the systematic errors of individual force fields by combining the results of simulations from multiple molecular force fields [121]. Protein-ligand relative binding free-energy calculations show that the consensus approach can reduce the RMSE from 1.7-1.9 kcal/mol to 1.5 kcal/mol by fusing the results of SAGE [122], GAFF [66], and CGenFF [91] force fields [121]. The implementation of the consensus approach can be performed using a simple averaging, weighted averaging, or machine-learning-based strategy. This strategy does not require any a priori knowledge and can improve the reliability of classical force fields by simply increasing the simulation time.

6. Recommendations for using cutting-edge schemes

Based on the above discussion, we present our recommendations for using the aforementioned cutting-edge schemes for improving the accuracy of classical force fields to describe nonbonded interactions when CHARMM [11] or Amber [9] force fields are used for simulations of biomolecules in aqueous solution, as shown in Table 1.

Table 1. Availability for using cutting-edge schemes to improve the description of nonbonded interactions for the CHARMM and Amber force fields

	CHARMM	Amber
Better charge modeling	RESP2: n.a. (Incompatible methods of calculating atomic charges)	RESP2: available
Additional virtual atoms	water: validation needed (TIP4P-FB, OPC and OPC3-pol) metal ions: validation needed halogen bonds: available (CGenFF)	water: available (OPC), validation needed (TIP4P-FB and OPC3-pol) metal ions: validation needed halogen bonds: n.a. (No relevant studies available at this time)
Larger VDW parameter space	metal ions: validation needed	metal ions: validation needed
NBFIX improvements	biomolecules and drug-like molecules: available (CUFIX, CHARMM36-WYF and CHARMM36m-NBF/SBF) biomolecules and drug-like molecules: available (CUFIX)	biomolecules and drug-like molecules: available (CUFIX)
Indirect chemical perception	drug-like molecules: available (CGenFF)	drug-like molecules: available (Boulanger et al. 2018)
Direct chemical perception	drug-like molecules: n.a. (No relevant studies available at this time)	drug-like molecules: available (OpenFF)
Consensus approach	available	

7. Conclusion

Despite the wide range of applications achieved by classical force fields in molecular simulations, their functional forms limit the ability to describe nonbonded interactions. The development of polarizable and machine-learning force fields in recent years has presented considerable challenges to classical force fields, and the necessity of continuously improving classical force fields remains a subject of intense debate. This review summarizes recent methodological developments aimed at improving the description of nonbonded interactions by classical force fields, and reveals that interactions such as metal ion-ligand coordination, cation-π, salt bridges, and halogen bonding can indeed be accurately described within the framework of classical force fields.

At the same time, we propose three major advantages of the classical force fields over the polarizable and the machine-learning force fields:

- High computational efficiency: all the methods mentioned in this paper operate within the functional framework of the classical force fields, which can be directly used with a GPU-based MD engine to perform simulations at the microsecond timescale with a 2 fs (or 4 fs, if hydrogen-mass repartitioning [123] is used) step size for molecular assemblies with more than 100,000 atoms. This efficiency is much higher than that of polarizable and the machine-learning force fields;
- High transferability: the parameters obtained by many of the methods mentioned in this paper can serve as drop-in improvements to existing standard force fields or can be used with only a simple validation (Table 1). In addition, for some new small molecules, a reasonable initial guess can usually be made from the existing default parameters without the need to re-parameterize. In contrast, machine-learning force fields require extensive testing and fine-tuning for different molecular assemblies. Parameter transferability in polarizable force fields likely exceeds that in machine-learning force fields but remains considerably below that in classical force fields due to the introduction of polarization-related parameters;
- Ease of parameterization: even for molecular assemblies where no force field parameter is available, parameterizing them for the system under study is comparatively straightforward. For example, (semi-)automated parameterization can be readily achieved using established tools including Force Field Toolkit (ffTK) [124], General AMBER Force Field (GAFF) [66], ForceBalance [81,125], and ParaMol [126]. Machine-learning force fields, on the other hand, require complex retraining or parameter fitting processes. Parameterization of polarizable force fields, historically highly challenging, is now moderately simplified by advanced tools such as Poltype [127] for the AMOEBA [9,10] polarizable force field.

Collectively, we believe that the existing classical force fields possess irreplaceable advantages in the study of biomolecule systems, given their significant untapped potential in accurately describing nonbonded interactions. By further improving the accuracy of the classical force fields, they are expected to play an important role in the fields of biomolecule simulations, drug screening and materials science. With the rapid development of computer hardware and software, we expect that in the future, simulations of whole viruses and cells using accurate classical force fields will become a widely performed, routine tool for biochemical studies.

Notes

The authors declare no competing financial interest.

Acknowledgments

This study was supported by the National Natural Science Foundation of China (22473062, 22374082, 22293032 and 22373051) and the Natural Science Foundation of Tianjin (23JCQNJC01420) and the Fundamental Research Funds for the Central Universities (020-63253140, 63251115).

References

[1] Shaw D.E., Maragakis P., Lindorff-Larsen K., Piana S., Dror R.O., Eastwood M.P., Bank J.A., Jumper J.M., Salmon J.K. and Shan Y., Atomic-level characterization of the structural dynamics of proteins. *Science*, **330** (6002) (2010), 341-346.

[2] Dror R.O., Dirks R.M., Grossman J., Xu H. and Shaw D.E., Biomolecular simulation: a computational microscope for molecular biology. *Annu. Rev. Biophys*., **41** (1) (2012), 429-452.

[3] Karplus M. and McCammon J.A., Molecular dynamics simulations of biomolecules. *Nat. Struct. Biol*., **9** (9) (2002), 646-652.

[4] Hospital A., Goñi J.R., Orozco M. and Gelpí J.L., Molecular dynamics simulations: advances and applications. *Adv. Appl. Bioinform. Chem*., **8** (2015), 37-47.

[5] Van Der Spoel D., Lindahl E., Hess B., Groenhof G., Mark A.E. and Berendsen H.J., GROMACS: fast, flexible, and free. *J. Comput. Chem*., **26** (16) (2005), 1701-1718.

[6] Ponder J.W. and Case D.A., Force fields for protein simulations. *Adv. Protein Chem*., **66** (2003), 27-85.

[7] Mu J., Liu H., Zhang J., Luo R. and Chen H.-F., Recent force field strategies for intrinsically disordered proteins. *J. Chem. Inf. Model*., **61** (3) (2021), 1037-1047.

[8] Choi T., Li Z., Song G. and Chen H.-F., Comprehensive comparison and critical assessment of RNA-specific force fields. *J. Chem. Theory Comput*., **20** (6) (2024), 2676-2688.

[9] Cornell W.D., Cieplak P., Bayly C.I., Gould I.R., Merz Jr K., Ferguson D., Spellmeyer D., Fox T., Caldwell J. and Kollman P., A new force field for molecular mechanical simulation of nucleic acids and proteins. *J. Am. Chem. Soc.*, **117** (1995), 5179-5197.

[10] Tian C., Kasavajhala K., Belfon K.A., Raguette L., Huang H., Migues A.N., Bickel J., Wang Y., Pincay J., Wu Q. and Wang L., ff19SB: amino-acid-specific protein backbone parameters trained against quantum mechanics energy surfaces in solution. *J. Chem. Theory Comput*., **16** (1) (2019), 528-552.

[11] MacKerell Jr A.D., Bashford D., Bellott M., Dunbrack Jr R.L., Evanseck J.D., Field M.J., Fischer S., Gao J., Guo H., Ha S., All-atom empirical potential for molecular modeling and dynamics studies of proteins. *J. Phys. Chem. B*, **102** (18) (1998), 3586-3616.

[12] Huang J., Rauscher S., Nawrocki G., Ran T., Feig M., De Groot B.L., Grubmüller H. and MacKerell Jr A.D., CHARMM36m: an improved force field for folded and intrinsically disordered proteins. *Nat. Methods*, **14** (1) (2017), 71-73.

[13] Jorgensen W.L., Maxwell D.S. and Tirado-Rives J., Development and testing of the OPLS all-atom force field on conformational energetics and properties of organic liquids. *J. Am. Chem. Soc*., **118** (45) (1996), 11225-11236.

[14] Robertson M.J., Tirado-Rives J. and Jorgensen W.L., Improved peptide and protein torsional energetics with the OPLS-AA force field. *J. Chem. Theory Comput*., **11** (7) (2015), 3499-3509.

[15] Wang L., Berne B. and Friesner R.A., On achieving high accuracy and reliability in the calculation of relative protein–ligand binding affinities. *Proc. Natl. Acad. Sci. U.S.A*., **109** (6) (2012), 1937-1942.

[16] Limongelli V., Marinelli L., Cosconati S., La Motta C., Sartini S., Mugnaini L., Da Settimo F., Novellino E. and Parrinello M., Sampling protein motion and solvent effect during ligand binding. *Proc. Natl. Acad. Sci. U.S.A*., **109** (5) (2012), 1467-1472.

[17] Vendruscolo M. and Dobson C.M., Protein dynamics: Moore's law in molecular biology. *Curr. Biol*., **21** (2) (2011), R68–R70.

[18] Lindorff-Larsen K., Piana S., Dror R.O. and Shaw D.E., How fast-folding proteins fold. *Science*, **334** (6055) (2011), 517-520.

[19] Cubero E., Luque F.J. and Orozco M., Is polarization important in cation–π interactions? *Proc. Natl. Acad. Sci. U.S.A*., **95** (11) (1998), 5976-5980.

[20] Jing Z., Liu C., Cheng S.Y., Qi R., Walker B.D., Piquemal J.-P. and Ren P., Polarizable force fields for biomolecular simulations: recent advances and applications. *Annu. Rev. Biophys*., **48** (1) (2019), 371-394.

[21] Chen J. and Martínez T.J., QTPIE: charge transfer with polarization current equalization. A fluctuating charge model with correct asymptotics. *Chem. Phys. Lett*., **438** (4-6) (2007), 315-320.

[22] Baker C.M., Polarizable force fields for molecular dynamics simulations of biomolecules. *Wiley Interdiscip. Rev. Comput. Mol. Sci*., **5** (2) (2015), 241-254.

[23] Cisneros G.A., Karttunen M., Ren P. and Sagui C., Classical electrostatics for biomolecular simulations. *Chem. Rev*., **114** (1) (2014), 779-814.

[24] Demerdash O., Wang L.P. and Head-Gordon T., Advanced models for water simulations. *Wiley Interdiscip. Rev. Comput. Mol. Sci*., **8** (1) (2018), e1355.

[25] Lemkul J.A., Huang J., Roux B. and MacKerell Jr A.D., An empirical polarizable force field based on the classical Drude oscillator model: development history and recent applications. *Chem. Rev*., **116** (9) (2016), 4983-5013.

[26] Mobley D.L. and Gilson M.K., Predicting binding free energies: frontiers and benchmarks. *Annu. Rev. Biophys*., **46** (1) (2017), 531-558.

[27] Zhang Y., Wang H., Chen W., Zeng J., Zhang L. and Wang H., DP-GEN: a concurrent learning platform for the generation of reliable deep learning based potential energy models. *Comput. Phys. Commun*., **253** (2020), 107206.

[28] Lopes P.E., Huang J., Shim J., Luo Y., Li H., Roux B. and MacKerell Jr A.D., Polarizable force field for peptides and proteins based on the classical Drude oscillator. *J. Chem.*

Theory Comput., **9** (12) (2013), 5430-5449.

[29] Unke O.T., Chmiela S., Sauceda H.E., Gastegger M., Poltavsky I., Schütt K.T., Tkatchenko A. and Müller K.-R., Machine learning force fields. *Chem. Rev*., **121** (16) (2021), 10142-10186.

[30] Pietrek L.M., Stelzl L.S. and Hummer G., Structural ensembles of disordered proteins from hierarchical chain growth and simulation. *Curr. Opin. Struct. Biol*., **78** (2023), 102501.

[31] Li N., Gao Y., Qiu F. and Zhu T., Benchmark force fields for the molecular dynamic simulation of G-quadruplexes. *Molecules*, **26** (17) (2021), 5379.

[32] Wang W., Yan D., Cai Y., Xu D., Ma J. and Wang Q., General charge transfer dipole model for AMOEBA-like force fields. *J. Chem. Theory Comput*., **19** (9) (2023), 2518-2534.

[33] Qu X., Dong L., Si Y., Zhao Y., Wang Q. and Su P., Reliable prediction of the protein–ligand binding affinity using a charge penetration corrected AMOEBA force field: a case study of drug resistance mutations in Abl kinase. *J. Chem. Theory Comput*., **18** (3) (2022), 1692-1700.

[34] Lin X., Wang W., He B., Li J., Wang Q. and Ma J., Transport parameters for combustion species based on cAMOEBA polarizable force field. *J. Chem. Theory Comput*., **19** (11) (2023), 3237-3250.

[35] Deng S., Wang Q. and Ren P., Estimating and modeling charge transfer from the SAPT induction energy. *J. Comput. Chem*., **38** (26) (2017), 2222-2231.

[36] Dong X., Yuan X., Song Z. and Wang Q., The development of an AMBER-compatible organosilane force field for drug-like small molecules. *Phys. Chem. Chem. Phys*., **23** (22) (2021), 12582-12591.

[37] Li P., Song L.F. and Merz Jr K.M., Systematic parameterization of monovalent ions employing the nonbonded model. *J. Chem. Theory Comput*., **11** (4) (2015), 1645-1657.

[38] Li P., Song L.F. and Merz Jr K.M., Parameterization of highly charged metal ions using the 12-6-4 LJ-type nonbonded model in explicit water. *J. Phys. Chem. B*, **119** (3) (2015), 883-895.

[39] Ren P. and Ponder J.W., Polarizable atomic multipole water model for molecular mechanics simulation. *J. Phys. Chem. B*, **107** (24) (2003), 5933-5947.

[40] Chu H., Peng X., Li Y., Zhang Y., Min H. and Li G., Polarizable atomic multipole-based force field for DOPC and POPE membrane lipids. *Mol. Phys*., **116** (7-8) (2018), 1037-1050.

[41] Lamoureux G. and Roux B., Modeling induced polarization with classical Drude oscillators: theory and molecular dynamics simulation algorithm. *J. Chem. Phys*., **119** (6) (2003), 3025-3039.

[42] Huang J., Lopes P.E., Roux B. and MacKerell Jr A.D., Recent advances in polarizable force fields for macromolecules: microsecond simulations of proteins using the classical Drude oscillator model. *J. Phys. Chem. Lett*., **5** (18) (2014), 3144-3150.

[43] Smith J.S., Isayev O. and Roitberg A.E., ANI-1: an extensible neural network potential with DFT accuracy at force field computational cost. *Chem. Sci*., **8** (4) (2017), 3192-3203.

[44] Zhang L., Han J., Wang H., Car R. and E W., Deep potential molecular dynamics: a scalable model with the accuracy of quantum mechanics. *Phys. Rev. Lett*., **120** (14) (2018), 143001.

[45] Behler J. and Parrinello M., Generalized neural-network representation of high-dimensional potential-energy surfaces. *Phys. Rev. Lett*., **98** (14) (2007), 146401.

[46] Behler J., First principles neural network potentials for reactive simulations of large molecular and condensed systems. *Angew. Chem., Int. Ed*., **56** (42) (2017), 12828-12840.

[47] Lorentz H.A., Ueber die Anwendung des Satzes vom Virial in der kinetischen Theorie der Gase. *Ann. Phys*., **248** (1) (1881), 127-136.

[48] Brooks B.R., Brooks III C.L., Mackerell Jr A.D., Nilsson L., Petrella R.J., Roux B., Won Y., Archontis G., Bartels C., Boresch S., CHARMM: the biomolecular simulation program. *J. Comput. Chem*., **30** (10) (2009), 1545-1614.

[49] Vanommeslaeghe K. and Guvench O., Molecular mechanics. *Curr. Pharm. Des*., **20** (20) (2014), 3281-3292.

[50] Inakollu V.S., Geerke D.P., Rowley C.N. and Yu H., Polarisable force fields: what do they add in biomolecular simulations? *Curr. Opin. Struct. Biol*., **61** (2020), 182-190.

[51] Lenhard J., Stephan S. and Hasse H., On the history of the Lennard-Jones potential. *Ann. Phys*., **536** (6) (2024), 2400115.

[52] Wang X., Ramírez-Hinestrosa S., Dobnikar J. and Frenkel D., The Lennard-Jones potential: when (not) to use it. *Phys. Chem. Chem. Phys*., **22** (19) (2020), 10624-10633.

[53] Chipot C., Recent advances in simulation software and force fields: their importance in theoretical and computational chemistry and biophysics. *J. Phys. Chem. B*, **128** (49) (2024), 12023-12026.

[54] Li P., Roberts B.P., Chakravorty D.K. and Merz Jr K.M., Rational design of particle mesh Ewald compatible Lennard-Jones parameters for +2 metal cations in explicit solvent. *J. Chem. Theory Comput*., **9** (6) (2013), 2733-2748.

[55] Li P. and Merz Jr K.M., Taking into account the ion-induced dipole interaction in the nonbonded model of ions. *J. Chem. Theory Comput*., **10** (1) (2014), 289-297.

[56] Gresh N., Cisneros G.A., Darden T.A. and Piquemal J.-P., Anisotropic, polarizable molecular mechanics studies of inter- and intramolecular interactions and ligand–macromolecule complexes. A bottom-up strategy. *J. Chem. Theory Comput.*, **3** (6) (2007), 1960-1986.

[57] Lopes P.E., Roux B. and MacKerell Jr A.D., Molecular modeling and dynamics studies with explicit inclusion of electronic polarizability: theory and applications. *Theor. Chem. Acc*., **124** (1) (2009), 11-28.

[58] Liao Q., Kamerlin S.C.L. and Strodel B., Development and application of a nonbonded Cu^{2+} model that includes the Jahn–Teller effect. *J. Phys. Chem. Lett*., **6** (13) (2015), 2657-2662.

[59] Huggins D.J., Biggin P.C., Dämgen M.A., Essex J.W., Harris S.A., Henchman R.H., Khalid S., Kuzmanic A., Laughton C.A., Michel J., et al., Biomolecular simulations: from dynamics and mechanisms to computational assays of biological activity. *Wiley Interdiscip. Rev. Comput. Mol. Sci*., **9** (3) (2019), e1393.

[60] Gutiérrez I.S., Lin F.Y., Vanommeslaeghe K., Lemkul J.A., Armacost K.A., Brooks III C.L. and MacKerell Jr A.D., Parametrization of halogen bonds in the CHARMM

general force field: improved treatment of ligand–protein interactions. *Bioorg. Med. Chem.*, **24** (20) (2016), 4812-4825.

[61] Liu H., Fu H., Chipot C., Shao X. and Cai W., Accurate description of solvent-exposed salt bridges with a non-polarizable force field incorporating solvent effects. *J. Chem. Inf. Model.*, **62** (16) (2022), 3863-3873.

[62] Liu H., Fu H., Shao X., Cai W. and Chipot C., Accurate description of cation–π interactions in proteins with a nonpolarizable force field at no additional cost. *J. Chem. Theory Comput.*, **16** (10) (2020), 6397-6407.

[63] Breneman C.M. and Wiberg K.B., Determining atom-centered monopoles from molecular electrostatic potentials: the need for high sampling density in formamide conformational analysis. *J. Comput. Chem.*, **11** (3) (1990), 361-373.

[64] Schmidt M.W., Baldridge K.K., Boatz J.A., Elbert S.T., Gordon M.S., Jensen J.H., Koseki S., Matsunaga N., Nguyen K.A., Su S., General atomic and molecular electronic structure system. *J. Comput. Chem.*, **14** (11) (1993), 1347-1363.

[65] Bayly C.I., Cieplak P., Cornell W. and Kollman P.A., A well-behaved electrostatic potential-based method using charge restraints for deriving atomic charges: the RESP model. *J. Phys. Chem.*, **97** (40) (1993), 10269-10280.

[66] Wang J., Wolf R.M., Caldwell J.W., Kollman P.A. and Case D.A., Development and testing of a general AMBER force field. *J. Comput. Chem.*, **25** (9) (2004), 1157-1174.

[67] Cerutti D.S., Rice J.E., Swope W.C. and Case D.A., Derivation of fixed partial charges for amino acids accommodating a specific water model and implicit polarization. *J. Phys. Chem. B*, **117** (8) (2013), 2328-2338.

[68] Cerutti D.S., Swope W.C., Rice J.E. and Case D.A., ff14ipq: a self-consistent force field for condensed-phase simulations of proteins. *J. Chem. Theory Comput.*, **10** (10) (2014), 4515-4534.

[69] Schauperl M., Nerenberg P.S., Jang H., Wang L.-P., Bayly C.I., Mobley D.L. and Gilson M.K., Non-bonded force field model with advanced restrained electrostatic potential charges (RESP2). *Commun. Chem.*, **3** (1) (2020), 44.

[70] Dodda L.S., Vilseck J.Z., Tirado-Rives J. and Jorgensen W.L., 1.14* CM1A-LBCC: localized bond-charge corrected CM1A charges for condensed-phase simulations. J. *Phys. Chem. B*, **121** (15) (2017), 3864-3870.

[71] Dodda L.S., Vilseck J.Z., Cutrona K.J. and Jorgensen W.L., Evaluation of CM5 charges for nonaqueous condensed-phase modeling. *J. Chem. Theory Comput.*, **11** (9) (2015), 4273-4282.

[72] Kale S. and Herzfeld J., Natural polarizability and flexibility via explicit valency: the case of water. *J. Chem. Phys.*, **136** (8) (2012), 084109.

[73] Tu Y. and Laaksonen A., The electronic properties of water molecules in water clusters and liquid water. *Chem. Phys. Lett.*, **329** (3-4) (2000), 283-288.

[74] Dill K.A., Truskett T.M., Vlachy V. and Hribar-Lee B., Modeling water, the hydrophobic effect, and ion solvation. Annu. Rev. *Biophys. Biomol. Struct.*, **34** (1) (2005), 173-199.

[75] Izadi S., Anandakrishnan R. and Onufriev A.V., Building water models: a different approach. *J. Phys. Chem. Lett.*, **5** (21) (2014), 3863-3871.

[76] Piana S., Donchev A.G., Robustelli P. and Shaw D.E., Water dispersion interactions strongly influence simulated structural properties of disordered protein states. *J. Phys. Chem. B*, **119** (16) (2015), 5113-5123.

[77] Yu H. and van Gunsteren W.F., Accounting for polarization in molecular simulation. *Comput. Phys. Commun.*, **172** (2) (2005), 69-85.

[78] Izadi S. and Onufriev A.V., Accuracy limit of rigid 3-point water models. *J. Chem. Phys.*, **145** (7) (2016), 074501.

[79] Savelyev A. and MacKerell Jr A.D., All-atom polarizable force field for DNA based on the classical Drude oscillator model. *J. Comput. Chem.*, **35** (16) (2014), 1219-1239.

[80] Jorgensen W.L., Chandrasekhar J., Madura J.D., Impey R.W. and Klein M.L., Comparison of simple potential functions for simulating liquid water. *J. Chem. Phys.*, **79** (2) (1983), 926-980.

[81] Wang L.P., Martinez T.J. and Pande V.S., Building force fields: an automatic, systematic, and reproducible approach. J. *Phys. Chem. Lett.*, **5** (11) (2014), 1885-1891.

[82] Xiong Y., Izadi S. and Onufriev A.V., Fast polarizable water model for atomistic simulations. *J. Chem. Theory Comput.*, **18** (10) (2022), 6324-6333.

[83] Lamoureux G., Harder E., Vorobyov I.V., Roux B. and MacKerell Jr A.D., A polarizable model of water for molecular dynamics simulations of biomolecules. *Chem. Phys. Lett.*, **418** (1-3) (2006), 245-249.

[84] Li P. and Merz Jr K.M., Metal ion modeling using classical mechanics. *Chem. Rev.*, **117** (3) (2017), 1564-1686.

[85] Duarte F., Bauer P., Barrozo A., Amrein B.A., Purg M., Åqvist J. and Kamerlin S.C.L., Force field independent metal parameters using a nonbonded dummy model. *J. Phys. Chem. B*, **118** (16) (2014), 4351-4362.

[86] Jiang Y., Zhang H., Feng W. and Tan T., Refined dummy atom model of Mg^{2+} by simple parameter screening strategy with revised experimental solvation free energy. *J. Chem. Inf. Model.*, **55** (12) (2015), 2575-2586.

[87] Liao Q., Pabis A., Strodel B. and Kamerlin S.C.L., Extending the nonbonded cationic dummy model to account for ion-induced dipole interactions. *J. Phys. Chem. Lett.*, **8** (21) (2017), 5408-5414.

[88] Clark T., Hennemann M., Murray J.S. and Politzer P., Halogen bonding: the σ-hole: proceedings of "Modeling interactions in biomolecules II", Prague, September 5th–9th, 2005. *J. Mol. Model.*, **13** (2007), 291-296.

[89] Kolar M.H. and Hobza P., Computer modeling of halogen bonds and other σ-hole interactions. *Chem. Rev.*, **116** (9) (2016), 5155-5187.

[90] Jorgensen W.L. and Schyman P., Treatment of halogen bonding in the OPLS-AA force field: application to potent anti-HIV agents. *J. Chem. Theory Comput.*, **8** (10) (2012), 3895-3901.

[91] Vanommeslaeghe K., Hatcher E., Acharya C., Kundu S., Zhong S., Shim J., Darian E., Guvench O., Lopes P., Vorobyov I., CHARMM general force field: a force field for drug-like molecules compatible with the CHARMM all-atom additive biological force fields. *J. Comput. Chem.*, **31** (4) (2010), 671-690.

[92] Zhang Y., Jiang Y. and Peng J., Rational design of nonbonded point charge models for divalent metal cations with Lennard-Jones 12-6 potential. *J. Chem. Inf. Model.*, **61** (8) (2021),

4031-4044.

[93] Smith M., Li Z., Landry L., Merz Jr K.M. and Li P., Consequences of overfitting the van der Waals radii of ions. *J. Chem. Theory Comput*., **19** (7) (2023), 2064-2074.

[94] Song L.F., Sengupta A. and Merz K.M., Jr, Thermodynamics of transition metal ion binding to proteins. *J. Am. Chem. Soc*., **142** (13) (2020), 6365-6374.

[95] Turupcu A., Tirado-Rives J. and Jorgensen W.L., Explicit representation of cation–π interactions in force fields with 1/r4 nonbonded terms. *J. Chem. Theory Comput*., **16** (11) (2020), 7184-7194.

[96] Wang M., Xiong Q., Wang M., Lewis N.H.C., Ying D., Yan G., Hoenig E., Han Y., Lee O.-S., Peng G., et al., Lanthanide transport in angstrom-scale MoS2-based two-dimensional channels. *Sci. Adv*., **10** (11) (2024), eadh1330.

[97] Leem A.Y. and Chen H., Simulating water adsorption in metal–organic frameworks with open metal sites using the 12-6-4 Lennard–Jones potential. *Mol. Simul*., **49** (11) (2023), 1135-1142.

[98] Sengupta A., Seitz A. and Merz Jr K.M., Simulating the chelate effect. *J. Am. Chem. Soc*., **140** (45) (2018), 15166–15169.

[99] Riniker S., Fixed-charge atomistic force fields for molecular dynamics simulations in the condensed phase: an overview. *J. Chem. Inf. Model*., **58** (3) (2018), 565-578.

[100] Luo Y. and Roux B., Simulation of osmotic pressure in concentrated aqueous salt solutions. *J. Phys. Chem. Lett*., **1** (1) (2010), 183-189.

[101] Yoo J. and Aksimentiev A., Improved parameterization of amine–carboxylate and amine–phosphate interactions for molecular dynamics simulations using the CHARMM and AMBER force fields. *J. Chem. Theory Comput*., **12** (1) (2016), 430-443.

[102] Yoo J. and Aksimentiev A., Improved parametrization of Li^+, Na^+, K^+, and Mg^{2+} ions for all-atom molecular dynamics simulations of nucleic acid systems. *J. Phys. Chem. Lett*., **3** (1) (2012), 45-50.

[103] Yoo J. and Aksimentiev A., New tricks for old dogs: improving the accuracy of biomolecular force fields by pair-specific corrections to non-bonded interactions. Phys. *Chem. Chem. Phys*., **20** (13) (2018), 8432-8449.

[104] Fu H., Chen H., Wang X.A., Chai H., Shao X., Cai W. and Chipot C., Finding an optimal pathway on a multidimensional free-energy landscape. *J. Chem. Inf. Mode*l., **60** (11) (2020), 5366-5374.

[105] Fu H., Zhang H., Chen H., Shao X., Chipot C. and Cai W., Zooming across the free-energy landscape: shaving barriers, and flooding valleys. *J. Phys. Chem. Lett*., **9** (16) (2018), 4738-4745.

[106] Liu H., Fu H., Chipot C., Shao X. and Cai W., Accuracy of alternate nonpolarizable force fields for the determination of protein–ligand binding affinities dominated by cation–π interactions. *J. Chem. Theory Comput*., **17** (7) (2021), 3908-3915.

[107] Fu H., Zhou Y., Jing X., Shao X. and Cai W., Meta-analysis reveals that absolute binding free-energy calculations approach chemical accuracy. *J. Med. Chem*., **65** (19) (2022), 12970-12978.

[108] Bian H., Shao X., Chipot C., Cai W. and Fu H., A formally exact method for high-throughput absolute binding-free-energy calculations. *Nat. Comput. Sci*., (2025).

[109] Mobley D.L., Bannan C.C., Rizzi A., Bayly C.I., Chodera J.D., Lim V.T., Lim N.M., Beauchamp K.A., Slochower D.R., Shirts M.R., Escaping atom types in force fields using direct chemical perception. *J. Chem. Theory Comput*., **14** (11) (2018), 6076-6092.

[110] Boulanger E., Huang L., Rupakheti C., MacKerell Jr A.D. and Roux B., Optimized Lennard-Jones parameters for druglike small molecules. *J. Chem. Theory Comput*., **14** (6) (2018), 3121-3131.

[111] Harder E., Damm W., Maple J., Wu C., Reboul M., Xiang J.Y., Wang L., Lupyan D., Dahlgren M.K., Knight J.L., OPLS3: a force field providing broad coverage of drug-like small molecules and proteins. *J. Chem. Theory Comput*., **12** (1) (2016), 281-296.

[112] Lu C., Wu C., Ghoreishi D., Chen W., Wang L., Damm W., Ross G.A., Dahlgren M.K., Russell E., Von Bargen C.D., OPLS4: improving force field accuracy on challenging regimes of chemical space. *J. Chem. Theory Comput*., **17** (7) (2021), 4291-4300.

[113] Damm W., Dajnowicz S., Ghoreishi D., Yu Y., Ganeshan K., Madin O., Rudshteyn B., Hu R., Wu M., Shang Y., OPLS5: addition of polarizability and improved treatment of metals. *ChemRxiv*, (2024).

[114] Du J., Zhang S., Wu G., Moura J.M.F. and Kar S., Topology adaptive graph convolutional networks. *arXiv*, (2017), 1710.10370.

[115] Zhang J., Atom typing using graph representation learning: how do models learn chemistry? *J. Chem. Phys*., **156** (20) (2022), 204108.

[116] Caleman C., Van Maaren P.J., Hong M., Hub J.S., Costa L.T. and Van Der Spoel D., Force field benchmark of organic liquids: density, enthalpy of vaporization, heat capacities, surface tension, isothermal compressibility, volumetric expansion coefficient, and dielectric constant. *J. Chem. Theory Comput.*, **8** (1) (2012), 61-74.

[117] Henriksen N.M., Fenley A.T. and Gilson M.K., Computational calorimetry: high-precision calculation of host–guest binding thermodynamics. *J. Chem. Theory Comput*., **11** (9) (2015), 4377-4394.

[118] Kenney I.M., Beckstein O. and Iorga B.I., Prediction of cyclohexane–water distribution coefficients for the SAMPL5 data set using molecular dynamics simulations with the OPLS-AA force field. *J. Comput.-Aided Mol. Des*., **30** (2016), 1045-1058.

[119] Rocklin G.J., Boyce S.E., Fischer M., Fish I., Mobley D.L., Shoichet B.K. and Dill K.A., Blind prediction of charged ligand binding affinities in a model binding site. *J. Mol. Biol*., **425** (22) (2013), 4569-4583.

[120] Wang Y., Fass J., Kaminow B., Herr J.E., Rufa D., Zhang I., Pulido I., Henry M., Macdonald H.E.B., Takaba K., End-to-end differentiable construction of molecular mechanics force fields. *Chem. Sci*., **13** (41) (2022), 12016-12033.

[121] Hahn D.F., Gapsys V., de Groot B.L. and Mobley D.L., Current state of open source force fields in protein–ligand binding affinity predictions. *J. Chem. Inf. Model*., **64** (13) (2024), 5063-5076.

[122] Boothroyd S., Behara P.K., Madin O.C., Hahn D.F., Jang H., Gapsys V., Wagner J.R., Horton J.T., Dotson D.L., Thompson M.W., Development and benchmarking of Open Force Field

2.0.0: the Sage small molecule force field. *J. Chem. Theory Comput.*, **19** (11) (2023), 3251-3275.

[123] Hopkins C.W., Le Grand S., Walker R.C. and Roitberg A.E., Long-time-step molecular dynamics through hydrogen mass repartitioning. *J. Chem. Theory Comput.*, **11** (4) (2015), 1864-1874.

[124] Mayne C.G., Saam J., Schulten K., Tajkhorshid E. and Gumbart J.C., Rapid parameterization of small molecules using the force field toolkit. *J. Comput. Chem.*, **34** (32) (2013), 2757-2770.

[125] Wang L.P., Chen J. and Van Voorhis T., Systematic parametrization of polarizable force fields from quantum chemistry data. *J. Chem. Theory Comput.*, **9** (1) (2013), 452-460.

[126] Morado J., Mortenson P.N., Verdonk M.L., Ward R.A. and Essex J.W., Skylaris C.-K., Paramol: a package for automatic parameterization of molecular mechanics force fields. *J. Chem. Inf. Model.*, **61** (4) (2021), 2026-2047.

[127] Wu J.C., Chattree G. and Ren P., Automation of AMOEBA polarizable force field parameterization for small molecules. *Theor. Chem. Acc.*, **131** (2012), 1-11.